

FIG. 2. Group of closely spaced lines in the spectrum of Ta^{183}

life of Ta^{183} was measured by us from the decrease in intensity of the most intense line in the spectrum with 246 -kev energy. The value of 5.0 ± 0.4 days found by us is in good agreement with earlier

published results (5.2 days⁸ and 5.3 days⁹).

- 1 P. I. Lukirskii and O. I. Sumbaev, *Izv. Akad. Nauk SSSR Ser. Fiz.* 20, 903 (1956).
- 2 Link, West and DuMond, *Phys. Rev.* 77, 475 (1950).
- 3 Bashilov, Anton'eva and Dzhelepov, *Izv. Akad. Nauk SSSR Ser. Fiz.* 16, 264 (1952).
- 4 M. W. Johns and S. V. Nablo, *Phys. Rev.* 96, 1599 (1954).
- 5 Baggerly, Marmier, Boehm and DuMond, *Phys. Rev.* 100, 1364 (1955).
- 6 Glazunov, Dzhelepov and Khol'nov, *Iszv. Akad. Nauk SSSR Ser. Fiz.* 19, 294 (1955).
- 7 Muller, Hoyt, Klein and DuMond, *Phys. Rev.* 88, 775 (1952).
- 8 Murray, Boehm, Marmier and DuMond, *Phys. Rev.* 97, 1007 (1955).
- 9 E. der Mateosian, *Phys. Rev.* 97, 1023 (1955).
- 10 J. W. M. DuMond, *Beta and Gamma-Ray Spectroscopy*. Edited by Kai Siegban (1955) (Interscience Publishers Inc., New York; p. 126).

Translated by F. Ajzenberg-Selove
54

Structure of the Periphery of Extensive Atmospheric Cosmic Ray Showers

IU. N. ANTONOV, IU. N. VAVILOV, G. T. ZATSEPIN,
A. A. KUTUZOV, IU. V. SKVORTSOV, G. B. KRISTIENSEN
P. N. Lebedev Physical Institute, Academy of Sciences, USSR
(Submitted to JETP editor August 14, 1956)
J. Exptl. Theoret. Phys. (U.S.S.R.) 32, 227-240 (February, 1957)

An investigation of the lateral distribution of various components of extensive showers at their periphery (200-800 m from the axis) has been carried out. The data on the lateral distribution indicate that the contribution of the shower periphery to the total shower particle flux is significant.

The lateral distribution of the electron component at the periphery can be explained by means of the theory of multiple Coulomb scattering. Coulomb scattering also plays an important role in the divergence of the penetrating particles (μ -mesons); however the angles of emission in the elementary events of nuclear cascade processes of π^\pm -mesons which give rise to μ -mesons can apparently also lead to this type of divergence of μ -mesons.

An investigation of the intensity of the primary cosmic radiation at very high energies (10^{16} - 10^{17} ev) was also carried out.

A DETAILED investigation of the peripheral regions of extensive atmospheric showers is of considerable interest from the point of view of elucidating the qualitative characteristic features of the nuclear-cascade process which forms the foundation of the development of the shower. At the same time such an investigation also turns out to be necessary for the determination both of the total number of particles in the shower and of the

ratios of the various components of the shower at any given depth of the atmosphere.

For the investigation of the periphery of showers, experimental arrangements are used involving counter systems situated at large distances D from each other which lead to a very large effective area of the recording system (of order D^2). This enables us to investigate the intensity of the primary cosmic radiation for ultra-high energies.

Up until now only a relatively small number of papers¹⁻⁵ has been published devoted to the study of the periphery of extensive atmospheric showers.

The majority of these papers (with the exception of that of Eidus et al.⁵ describe work carried out by not very modern methods (the method of the correlation curve) which yield only qualitative results.⁶

In 1948 experiments were carried out in the Pamir³ to determine the extent of the spatial distribution of the penetrating particles in extensive showers. Since these experiments were not published we shall describe them briefly.

Three groups of counters, each of 0.4 m² in area, were placed at a distance of approximately 2 m from each other and were separately screened by lead filters 22 cm thick. The number of coincidences between these three groups was determined.*

At the same time the number of coincidences was determined between this system of counter and either a group of counters shielded by lead or an uncovered counter of small area situated nearby.

We present below the experimental data:

	$C_3(\Sigma\Sigma\Sigma)$	$C_4(\Sigma\Sigma\Sigma\Sigma)$	$C_4(\Sigma\Sigma\Sigma, \sigma)$
Number of coincidences	119	32	20
Time of measurement (in hours)	18	8	10
	$\Sigma = 0.4 \text{ m}^2$	$\sigma = 0.01 \text{ m}^2$	

The counters of area Σ are screened by 22 cm of Pb. The counter of area σ is uncovered.

From these data the mean flux density penetrating particles reaching the screened counters was determined, and also the mean total flux density of charged particles over the uncovered counter. The ratio of these densities turned out to be equal to 0.06 for the central regions of the shower instead of the value 0.01 found in earlier investigations.^{7,8}

This result was naturally interpreted as a slower rate of falling off from the core towards the periphery of the flux densities of penetrating particles as compared to the flux densities of electrons.

Further fluxes of penetrating particles were observed over distances up to 500 m from the shower core. We present below the data on the number of coincidences between groups of counters for various distances D between them both with screening (upper line) and without it:

	$D = 2 \text{ m}$	$D = 500 \text{ m}$
$C_4(0.4, \overline{08}; 0.4, \overline{08}) \text{ hour}^{-1}$	(32.4 ± 2.2)	(0.52 ± 0.11)
$C_4(0.4, 08; 0.4, 08) \text{ hour}^{-1}$	(1892 ± 43)	(3.64 ± 0.54)

These data showed that at the periphery of the shower, the flux density of penetrating particles falls off more slowly than the flux density of all charged particles.

In order to make a detailed quantitative study of the showers, a new method was used for the first time during the summer and fall of 1950 and 1951 by participants in the Pamir expedition of the Academy of Sciences, USSR at an altitude of 3860 m above sea level. By means of hodoscopic arrangements, the flux densities of all charged particles and of penetrating particles separately were simultaneously recorded at several stations in the observation plane (the method of correlated hodoscopes).

DESCRIPTION OF THE APPARATUS AND THE EXPERIMENTAL METHOD

The apparatus was in the form of a hodoscopic system consisting of several (from 3 to 5) hodoscopic stations operating in correlation when traversed by an extensive atmospheric shower. The system is shown in Fig.1 where $D = 1000 \text{ m}$ and $d = 600 \text{ m}$.

At hodoscopic station 3, in addition to an indicator of flux densities, there was also placed a detector of penetrating particles which at the same time had sufficient sensitivity to detect particles

*According to the data obtained in the present work, such coincidences are produced principally by showers whose cores lie at distances of the order of several hundred meters from the experimental setup.

from nuclear disintegrations. A cross-section of the detector is given* in Fig. 2. Such a hodoscopic system recorded showers which gave coincidences between 6 groups of counters each 0.8 m^2 in area, half of which (3 groups) was situated at station 1 while the other half was situated at station 3.

The possibility of measuring the particle flux density at each of the stations over a wide range of densities was provided by using a set of hodoscopic counters of three different areas $\sigma = 330, 100, 18 \text{ cm}^2$. The use of 24 counters of a given area enables one to determine densities with an accuracy of the order of 30%.

In the Table below we present data on the number and the areas of the counters at the different stations.

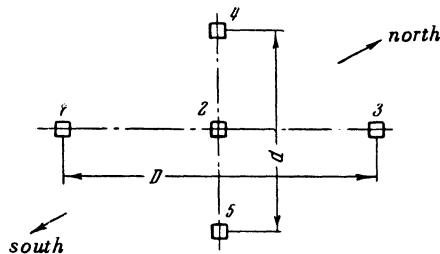


FIG. 1. Plan of the experimental arrangement. 1, 2, 3, 4, 5, are the hodoscopic stations. The distances are $D = 1000 \text{ m}$ and $d = 600 \text{ m}$.

At each hodoscopic station the hodoscopic counters were placed in a horizontal plane. The axes of all the counters in the whole hodoscopic system were oriented in the same direction parallel to the line 1-2-3.

The distance between the counters at any hodoscopic station was not less than half the diameter of these counters. As the analysis of the obtained data shows,⁹ such a distance is quite sufficient to avoid distortions in the measurement of particle flux densities which are due to the presence

Counter area, cm^2	Station number				
	1	2	3	4	5
330	72	48	$72 + \overline{60}$	48	48
100	24	24	24	24	24
18		24			

at the periphery of the shower of a relatively large number of diffusely scattered particles.

The whole system was controlled in the following manner. At each of stations 1 and 3, triple coincidence circuits were placed, into each channel of which were connected 24 counters of total area 0.8 m^2 (which were at the same time also connected to the hodoscope channels).

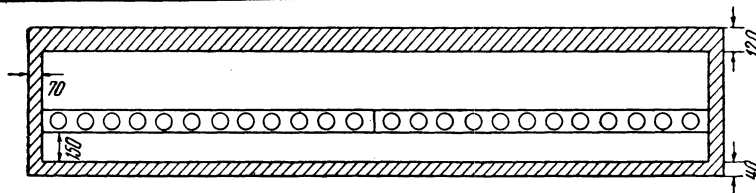


FIG. 2. Cross-section of the penetrating particle detector. The screening material is lead. The dimensions are given in mm. The screening of the counters at the ends is the same as at the sides.

*Next to the penetrating particle detector there was placed a group of 36 counters of dimensions $60 \times 550 \text{ mm}^2$ screened from above by 4 cm of Pb. On the basis of data on the flux densities of the particles in air, under 4 and under 12 cm of Pb (in the penetrating particle detector), the ratio of electron density under 4 cm of Pb to electron density in air was determined. This ratio turned out to be equal to 0.3 over the whole range of distances from the shower cores investigated by us. From this ratio we computed that the electron flux density under 12 cm of Pb must amount to 5×10^{-3} of their flux density in air. Since over the range of distances from the shower cores investigated by us the fraction of penetrating particles has a value of 0.1 or more (see the Section "Results" below) we may neglect the contribution due to electrons under 12 cm of Pb.

Whenever a triple coincidence took place, each circuit produced a shaped pulse at its output. Such pulses from stations 1 and 3 were transmitted along a high frequency cable to station 2 where a two-channel coincidence circuit recorded sixfold coincidences. Whenever sixfold coincidences occurred, the two-channel circuit produced a shaped pulse which was sent out along several cables to all the hodoscopic stations including 1 and 3. This pulse triggered the circuit controlling the hodoscope which emitted a controlling pulse to all the hodoscopic cells and which activated the photographic recording system.

The resolving time for the triple coincidence circuits was chosen as 3 microseconds. This, in particular, made allowance for the possible retardation of some particles with respect to others at the periphery of the shower.

The two-channel coincidence circuit which recorded the coincidence of pulses arriving from stations 1 and 3 had a resolving time $\tau = 5 \times 10^{-6}$ sec which guaranteed a high efficiency of recording all showers, including oblique ones, which caused the firing of counters in each of the six controlling groups. It is obvious that in order to record oblique showers it is necessary that τ should be approximately given by $\sim D/c = 3.3 \times 10^{-6}$ sec, where c is the velocity of light. The number of sixfold coincidences was equal to 0.4 pulses per hour.

The additional hodoscopic stations 2,4,5 easily enabled us to differentiate the true sixfold coincidences produced by the passage of a single shower consisting of a large number of particles from accidental coincidences which are primarily due to the passage of two independent showers containing a small number of particles through stations 1 and 3. With the circuit parameters chosen by us, the relative number of accidental sixfold coincidences* amounted to 20%.

The hodoscopes in the present experiment consisted of self-quenching counters of different dimensions (filled with a mixture of 70% argon and 30% ethylene at a pressure $p = 100$ mm of Hg) connected to hodoscopic cells of type GK-3.¹⁰

The inefficiency of the hodoscope as a whole was primarily determined by the inefficiency associated with the dead time of the counters connected to the hodoscope.

The resolving time of the hodoscopic cells had an average value of 30 microseconds with values for individual cells scattered between 10 and 40 microseconds. Such a resolving time guaranteed reliable operation of all the hodoscopic cells in spite of the appreciable (up to 5×10^{-6} sec) possible delays of the controlling pulse with respect to pulses from the counters (for example, at hodoscopic stations situated at a distance from the central station 2). On the other hand, such a resolving time gives not more than one accidental firing of the hodoscopic cell for each 1000 controlling pulses, which is (by a large factor) less than the frequency of firing of the cells due to particle fluxes even in the least energetic extensive atmospheric showers which are still to a noticeable

* The number of such coincidences increases as $\sigma^2 \kappa$, where $\kappa = 1.5$, and for areas of the order of 1 m^2 attains values comparable with the number of true coincidences which increases as $\sigma^2 - 1$.

extent registered by the apparatus.**

The experimental setup described above enabled us to determine the spatial distribution of all the charged particles and separately of the penetrating particles. It is evident that a complete solution of this problem requires the knowledge of the individual characteristics of the shower, i.e., the position of the core of each shower and the number of particles in it. In the most highly developed variant of the method of correlated hodoscopes¹¹ where the number of stations containing indicators of density is large the problem of determining the individual characteristics is dealt with separately from the problem of finding the spatial distribution. For the experimental setup under discussion these two problems turn out to be inseparable.

Let us consider the specific solution of these two problems in two cases: a) the hodoscopic system consists of three stations containing density indicators; b) the hodoscopic system consists of five such stations.

a) We denote by N the total number of particles in the shower and by $\rho(r) = kNf(r)$ the function giving the spatial distribution of the shower particles.*** Let ρ_1, ρ_2, ρ_3 be the particle flux

densities observed in a given shower at stations 1,2,3; and let r_1, r_2, r_3 be the distances from the shower core to stations 1,2,3.

Then on the basis of this notation and of Fig. 1, and also making use of the axial symmetry of the spatial distribution function of the shower particles, we can write the following system of equations relating the unknown quantities r_1, r_2, r_3, kN and the unknown function $f(r)$ to the quantities ρ_1, ρ_2, ρ_3 and the apparatus geometry

$$\rho_i = kNf(r_i) \quad (i = 1, 2, 3); \tag{1}$$

$$D^2 - 2 = r_1^2 + r_3^2 - 2r_2^2.$$

It is seen that this system of equations cannot be solved simultaneously with respect to r_1, r_2, r_3, kN and also with respect to $f(r)$. The function $f(r)$ must be found on the basis of additional data.

** In view of the large number of different elements in the experimental setup (600 counters were used in the investigation, of which 144 were used for the control circuit, and 600 hodoscopic cells GK-3 were also employed) particular attention was paid to monitoring the operation of the apparatus. All questions concerning the monitoring of the apparatus are dealt with in Khristiansen's thesis.⁹

*** k is a constant factor (see below).

Such additional data may be obtained if we consider the characteristics not of an individual shower but of the totality of showers recorded by the apparatus. Such characteristics are for example the spectra of particle densities at stations 1,2,3.

The above integral characteristics are sensitive only to the general character of the behavior of the spatial distribution function, since they are obtained by integrating the function $f(r)$ within certain limits (see below). Taking into account the results of the analysis of the correlation curve carried out by Skobel'tsyn,¹² it is useful to represent the dependence on r in the form $f(r) = r^{-n}$, where n is the parameter to be determined.

The quantity most sensitive to the value of n turns out to be the spectrum of particle flux densities at station 2 (see Ref. 9). This spectrum can be calculated theoretically for a given value of n and for a given form of the shower spectrum with respect to the number of particles $F(>N) \sim N^{-\kappa}$. If κ is determined in addition, then the theoretical characteristics obtained in this way may be compared with the corresponding experimental characteristics and from this one can determine the desired parameter n for the function $\rho(r) \sim 1/r^n$.

The solution of the problem of the individual shower characteristics for $\rho(r) = kN/r^n$ has the following form:

$$r_1 = (D/\sqrt{2}) [1 + (\rho_1/\rho_3)^{2/n} - 2(\rho_1/\rho_2)^{2/n}]^{-1/2} \text{ etc.}$$

$$kN = (D^n/2^{n/2}) [(1/\rho_1)^{2/n} + (1/\rho_3)^{2/n} - 2(1/\rho_2)^{2/n}]^{-n/2}. \quad (2)$$

b) Using the same notation, we can write the following equations which relate the individual shower characteristics and the spatial distribution function to the geometry of the apparatus and the particle flux densities produced over stations 1,2,3,4,5 (see Fig. 1)

$$\rho_i = kNf(r_i) \quad (i = 1 \dots 5) \quad (3)$$

$$D^2/2 = r_1^2 + r_3^2 - 2r_2^2,$$

$$d^2/2 = r_4^2 + r_5^2 - 2r_2^2.$$

We see that in this case one could formulate the problem of finding the spatial distribution function in a form which would depend on two parameters for each individual shower. In such a case, the above system of equations would enable us to obtain an analytic solution of the above problem.

However, such a solution of the problem for an individual shower in the case when the number of hodoscopic stations is small (as is the case in our arrangement) is not worth while for the following reasons. In each shower we obtain information on densities at several distances from the core. Thus the parameters of the desired distribution function will in each individual case be determined by the accidental combination of distances from the core selected in a given shower, and therefore will not give an overall picture of the spatial distribution function. This leads to the necessity of a statistical approach to the problem.*

The possibilities of applying the new method are due to our being able to identify each recorded shower in two independent ways, by utilizing data on observed flux densities of shower particles at all five stations.

We restrict ourselves to finding the spatial distribution function in the form $1/r^n$. Then for each recorded shower, Eq. (3) leads to two sets of values characterizing the number of particles and the position of the shower core

$$kN_I = (D^n/2^{n/2}) [(1/\rho_1)^{2/n} \quad (4)$$

$$+ (1/\rho_3)^{2/n} - 2(1/\rho_2)^{2/n}]^{-n/2};$$

$$kN_{II} = (d^n/2^{n/2}) [(1/\rho_4)^{2/n}$$

$$+ (1/\rho_5)^{2/n} - 2(1/\rho_2)^{2/n}]^{-n/2};$$

$$r_{2I} = (D/\sqrt{2}) [(\rho_2/\rho_1)^{2/n} + (\rho_2/\rho_3)^{2/n} - 2]^{-1/2};$$

$$r_{2II} = (d/\sqrt{2}) [(\rho_2/\rho_4)^{2/n} + (\rho_2/\rho_5)^{2/n} - 2]^{-1/2}.$$

On the basis of these formulas we can obtain the probability distributions for the numbers N_I, N_{II} in each individual shower if we know the distributions of $\rho_1 \dots \rho_5$. The index of the function n may evidently be found from the requirement of optimum overlapping of the distributions for N_I and N_{II} , and of the simultaneous optimum overlapping of the regions I and II of the possible points struck by the core of the shower. As has been mentioned earlier, it is not worthwhile to solve this problem for an individual shower. Therefore one should examine analogous data simultaneously for a large number of showers selected according to some definite criterion (approximate number of particles in the shower or the selected range of distances to the apparatus). In this way we shall average the ratios ρ_i/ρ_k appearing in

* We do not stress that the determination of the spatial distribution function for an individual shower is also impossible because of large errors in the determination of $\rho_1, \rho_2 \dots \rho_5$.

expressions (4) over the whole range of the practically continuously varying values of r . The index n may then evidently be found from the requirement of optimum overlapping of the sum of the distributions for N and also of the regions containing the points struck by the shower cores.

It should be noted that an approximate identification of each recorded shower is possible on the basis of an approximate value of n (for example, from the method of integral characteristics). Therefore, by means of the method described above, it is possible to determine the spatial distribution function in the form $1/r^n$ for various ranges of N and r and in this way to obtain an idea of the dependence of n on the ranges of N and r under investigation. The method of integral characteristics does not allow one to do this.

We note in conclusion that the determination of the spatial distribution of the penetrating component from the readings of the penetrating particle detector presents no difficulties if we know the individual characteristics of each recorded shower.

RESULTS

During the entire time of the experiment (1200 hours), approximately 500 cases of sixfold coincidences were recorded from which 370 cases which were in each case due to the passing of a single extensive atmospheric shower * were selected by examining the hodoscopic photographs.

The following stations participated in the recording of these extensive atmospheric showers:

Number of showers	Stations taking part in recording
80	1, 2, 3
70	1, 2, 3 and penetrating particle detector
120	1, 2, 3, 4
100	1, 2, 3, 4, 5 and penetrating particle detector

On the basis of the data obtained it is possible to determine the absolute intensity of extensive atmospheric showers containing a number of particles N larger than some given number. Indeed the number of sixfold coincidences may be represented by the expression

$$C_6 \frac{\text{---}}{\text{hour}} = A \int_0^\infty N^{-(\kappa+1)} \int_{s'}^\infty (1 - e^{-hN/r_1^n})^3 (1 - e^{-hN/r_2^n})^3 ds dN. \tag{A}$$

* The remaining coincidences, with the exception of one special case, apparently represent accidental coincidences caused by the passage of two independent showers of relatively small energies.

The quantity κ may be determined by the method of varying the areas of the counters.¹³ Since the controlling counters were connected to the hodoscope at the same time, we obtained several practically independent series of measurements of the number of showers by counters of different areas, which gave the average value $\kappa = 2.15 \pm 0.15$.

The constant A was then found by means of numerical integration over S and N . The expression for the absolute intensity of showers containing a number of particles greater than N obtained by the method described above has the form:

$$F(>N) = 1 \cdot 10^{11} \frac{1}{m^2 \cdot \text{hour} \cdot \text{sterad}} N^{-2.1}$$

In order to investigate the structure of the periphery of the recorded showers we utilized the methods described earlier.

In order to determine the form of the spatial distribution of charged particles, we plotted the spectra of the particle flux densities for each of stations 1,2,3,4,5 on the basis of the experimental data. The transition from the direct hodoscopic data on the number of counters which had fired to the values of ρ was carried out in the usual way (see for example Ref. 5).

We compared the experimental spectra obtained by us with the spectra calculated by means of numerical integration on the basis of different assumptions with respect to n and κ .⁹ Figure 3 shows experimental spectra of the flux densities at stations 1,2,3,4,5 and the theoretically calculated spectra of the flux densities at the same stations based on different assumptions* with respect to n and κ . As may be seen, there is good agreement between the experimental spectra of the flux densities at identical stations 1 and 3 and 4 and 5. The theoretically calculated spectra of the flux densities show a very strong dependence on n for station 2 and practically a complete lack of dependence on n for station 1 (or 3). As may be seen from the diagram, the theoretically calculated spectra using the values $n = 3$ and $\kappa = 2.1$ agree well with the experimental spectra both for station 2 and also for station 4 (or 5).

Figure 4 shows the range of distances from the shower core over which the exact shape of the function is averaged in constructing the spectra of the flux densities at the various stations. Figure 5 shows a spectrum with respect to the

*As calculations have shown, the assumptions made with respect to the form of $\rho(r)$ at small distances from the shower core play no significant role.

number of particles in the shower as given by the apparatus.

In constructing these spectra, r and N were determined by the experimental values of ρ_i with the index having the value $n = 3$ in accordance with Eqs. (2). The constant k was found on the assumption that

$$\rho(r) = kN / r^n \quad \text{for } r > R(n - 1),$$

$$\rho(r) = k_1 N e^{-r/R} r^{-1}$$

for $r < R(n - 1)$, $R = 80 \text{ m}$.

The curve $r^{-1} e^{-r/R}$ gives good agreement with the experimental curve of the spatial distribution of shower particles for $r < R(n - 1)$ and goes over smoothly into the function r^{-n} for $r > R(n - 1)$. From the conditions $kN/r^n = k_1 N e^{-r/R} r^{-1}$ for $r = R(n - 1)$ and $N = \int_0^\infty \rho(r) 2\pi r dr$ for $n = 3$ we obtain $k = 3$.

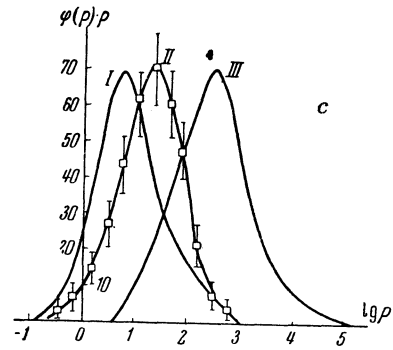


FIG. 3. Spectra of the densities of showers recorded at the different hodoscopic stations. $\lg \rho$ is plotted along the horizontal axis (ρ in units of $1/m^2$), the number of showers of density ρ in the interval ρ is plotted along the vertical axis— a —for stations 1,3; b —for stations 4,5; Δ and \blacktriangle are the experimental points for 1950 and 1951 for station 1, \circ and \bullet —the same for station 3, \times —the same for stations 4 and 5. In Figs. 3a and 3b the solid curves are theoretical curves for $n = 3$ and $\kappa = 2.1$; in Fig. 3c for station 2 the curves I, II, III are theoretical curves for $n = 2.6$, $n = 3$ and for $\rho(r)$ given by the cascade theory¹⁴; $\kappa = 2.1$, are the experimental data.

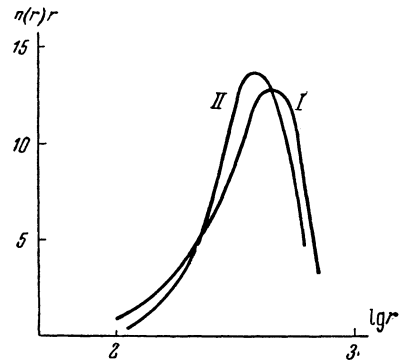
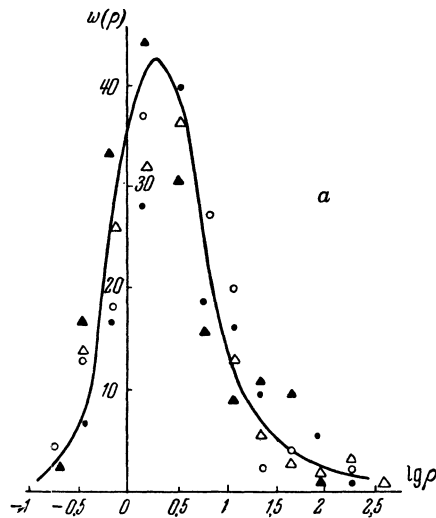


FIG. 4. Distances from the shower core to the hodoscopic stations. I is the distribution of distances to stations 1,2,3; II—the same for stations 1,3,4 (5).

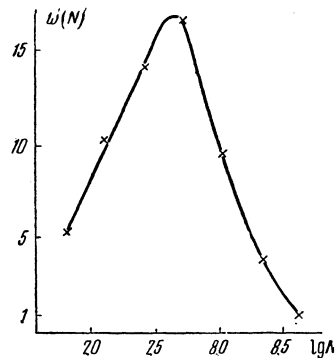
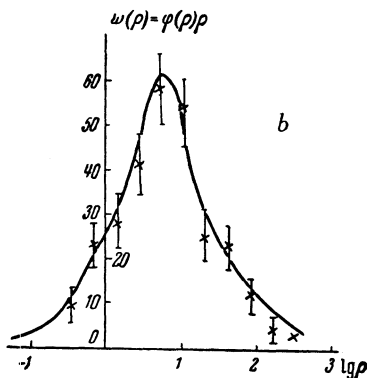


FIG. 5. The spectrum of recorded showers with respect to the number of particles.

In order to find the dependence of the index n on the number of particles in the shower N and on the distance r , we made use of the second method. In breaking up all the observed showers into groups belonging to different ranges of r and N preliminary values for the latter were obtained on the assumption $n = 3$. For showers belonging to each group we then determined the sums $\Sigma(N_I - N_{II})/\bar{N}$ for different values of the index n .* Here N_I is

the number of particles in a shower determined on the basis of the values of ρ_1, ρ_2, ρ_3 ; N_{II} is

the number of particles in a shower determined on the basis of ρ_4, ρ_5, ρ_2 .

The quantity $\Sigma \frac{N_I - N_{II}}{\bar{N}}$, regarded as a function of n , must show the following behavior: near the value $n = n_0$ which best of all characterizes the average behavior of the function $\rho(r)$, it must have two minima, and at the value $n = n_0$ it must have a relative maximum.**

We carried out the calculation for several discrete values of n in the neighborhood of the expected value $n = 3$. Figure 6 shows some of the results of these calculations.

As may be seen from the graphs and from the results of calculations, the index n which best characterizes the average behavior of the functions is in each case close to 3, and thus (within $\Delta n = \pm 0.2$) does not depend on the ranges of r and N over which the function $\rho(r)$ is averaged.

On the basis of the individual characteristics obtained by us, we also found the spatial distribution of the penetrating component. For the construction of this spatial distribution, the whole available range of distances was divided into a number of separate intervals, for each of which the average flux density of penetrating particles was found by using all the showers falling within this interval.

Since the distance between the shower core and the penetrating particle detector was determined with a fairly large error, we made allowance for the probability of those showers falling within the given interval which correspond to an average value \bar{r} belonging to other intervals. Figure 7 shows the spatial distribution of penetrating particles in showers with an average number of particles given by $\bar{N} \approx 10^8$.

If the spatial distribution of penetrating particles is represented by means of a power law $\sim r^{-n}$ then the use of the method of least squares will yield for showers with $\bar{N} \sim 10^7$ $n = 1.6 \pm 0.3$ and for showers with $\bar{N} \sim 10^8$ $n = 2.0 \pm 0.4$.

It is also of interest to find the fraction of penetration particles at various distances from the

**The existence of minima in the sum Σ near $n = n_0$ and not at $n = n_0$ is explained by the fact that the experimental values of ρ for each individual shower cannot exactly satisfy the distribution $\rho(r)$. They agree better with a distribution with an index n , which, although close to n_0 , is nevertheless different from it.

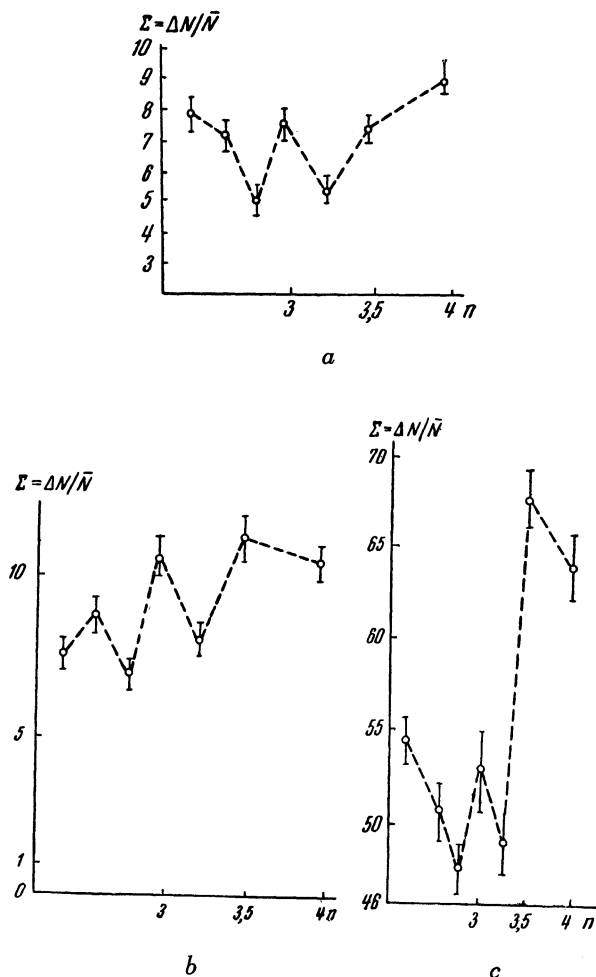


FIG. 6. The quantities $\Sigma(N_I - N_{II})/\bar{N}$ for showers with different ranges of r and N . a— $200\text{ m} < r < 600\text{ m}$, $5 \times 10^6 < N < 5 \times 10^7$; b— $400\text{ m} < r < 800\text{ m}$, $5 \times 10^6 < N < 5 \times 10^7$; c—for all the 100 showers each of which was simultaneously recorded at all five stations.

*Due to the lengthy calculations involved, we restricted ourselves to a comparison of two measurements of the number of particles, and did not compare measurements involving a change of axis.

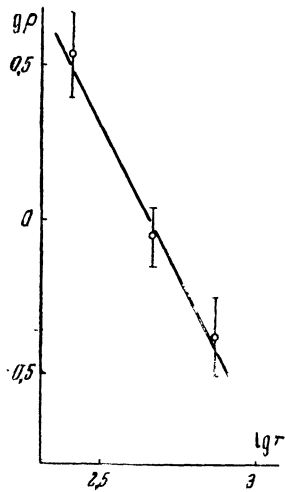


FIG. 7. The spatial distribution of penetrating particles (μ -mesons) for showers with the number of particles: $N \approx 10.8$

shower core. Since an indicator of the particle flux densities was situated at station 3, the fraction of penetrating particles could be easily determined as the average value of the ratio of the flux density of penetrating particles to the flux density of all charged particles taken over all the showers under consideration. Figure 8 gives the fraction of penetrating particles as a function of the distance from the shower core. It may be seen that the fraction of penetrating particle increases continuously as the distance from the core increases and reaches a value $\delta = 0.4$ at distances of the order of 800 m. At the same time it should be noted that the observed value of the fraction of penetrating particles signifies that in addition to μ -mesons and electrons in equilibrium with them, a considerable contribution to the flux density of charged particles up to distances of the order of 800 m is made by electrons of origin different from those which are in equilibrium with the μ -mesons. Figure 8 also gives for comparison the data of Eidus et al.⁵

The analysis of hodoscopic photographs obtained for the penetrating-particle detector shows that group firings of neighboring counters situated under a lead screen are extremely rare. The frequency of firings of two neighboring counters is in good agreement with the theoretically expected effect due to δ -electrons. At the same time, we observed three cases (in the total number of 100 investigated showers) in which more than three neighboring counters fired simultaneously. However, all these cases corresponded in general to a large density of penetrating particles (showers with a large N and a relatively small r). Thus

the group firings in these cases may be explained by the large density of penetrating particles and there is no need to suppose that they are caused by particles coming from nuclear disintegrations.

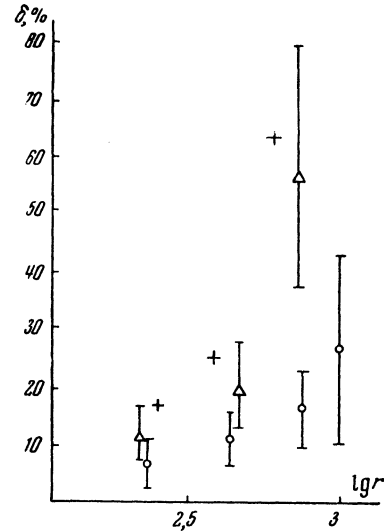


FIG. 8. The ratio of the number of penetrating particles (μ -mesons) to the number of all charged particles at different distances from the shower core. Δ —for showers with $N = 10^7$; \circ —for showers with $N = 10^8$; +—data for Ref. 5 for showers with $N \sim 10^7$ (at sea-level).

DISCUSSION OF RESULTS

The relatively slow falling off of the flux densities of all charged particles ($\sim 1/r^3$), and particularly of the penetrating particles ($\sim 1/r^2$) at the periphery of the shower, points to the important contribution of the periphery to the total number of shower particles and particularly to the number of penetrating particles in it.

Making use of the present data, and also of the data of Refs. 11 and 15, we can construct curves which characterize the contribution of the different parts of the shower situated at different distances from its core to the total number of shower particles. Such curves are given in Fig. 9. The fraction of penetrating particles in the hole shower (including its periphery) obtained from these curves is not less than 5%, which exceeds by severalfold the previous estimates¹⁵ of this quantity for mountain altitudes.

At the same time the slow falling off of the flux densities of shower particles at the periphery shows that a study of the periphery is absolutely essential for the correct investigation of the problem of the spatial divergence of particles in a nuclear-cascade process. The spatial divergence

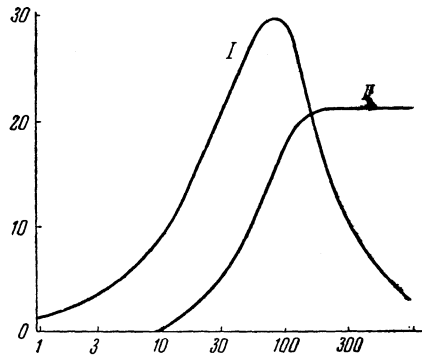


FIG. 9. Contribution of the different parts of the shower to the total number of shower particles of different kinds: *I*—for electrons, *II*—for μ -mesons. The density of shower particles multiplied by r^2 is plotted along the vertical axis, the distance r from the shower core in meters is plotted along the horizontal axis.

of charged particles in a shower may be due to the following causes: 1) the emission at relatively large angles in individual nuclear interaction events either of the directly recorded particles or of their predecessors (π^\pm -mesons if we are considering μ -mesons); 2) Coulomb scattering of particles by nuclei of atoms of air; 3) their deflection under the influence of the earth's magnetic field. These various causes play different roles in the divergence of shower particles of different kinds.

Let us first examine this question for that part of the electron component at the periphery of the shower which is not caused by the observed flux of μ -mesons, i.e., which is not of "equilibrium" nature. The spatial distribution of this "non-equilibrium" electron component can evidently be obtained from the distributions of all the charged particles and of the penetrating particles

$$\rho_{el}(r) \sim \frac{1}{r^3} - k \frac{1}{r^2},$$

where k is a coefficient which takes into account the flux density of μ -mesons and of electrons in equilibrium with them. Figure 10 shows the spatial distribution of the electrons. The coefficient k has been calculated for a μ -meson energy equal to 10^9 ev.*

These electrons are the cascade descendants of γ -quanta originating in the decay of π^0 -mesons generated in nuclear collisions. In our further discussion of the spatial distribution of electrons, we shall have in mind only this fraction of the

* The value of this coefficient depends very little on the μ -meson energy. We used the average energy of the μ -mesons in a shower as taken from Cocconi et al.¹⁵

electrons. As is well known, electrons in electron-photon avalanches undergo considerable scattering by charged nuclei of atoms of air. Their spatial distribution at large distances from the core originating in this manner apparently has been calculated most accurately in recent papers by Nishimura and Kamata.¹⁶

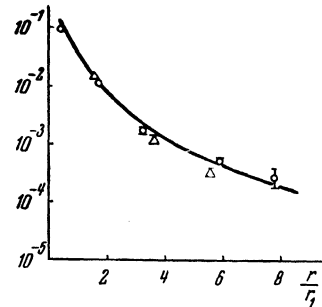


FIG. 10. The spatial distribution of the electron component which is not in equilibrium with the penetrating particles (μ -mesons) at the periphery of the shower— Δ —experimental points for $N = 10, 7$, \circ —for $N = 10, 8$. The solid curve is the theoretical spatial distribution of electrons in an electron-photon avalanche with $S = 1.0$ (Nishimura and Kamata). The distance from the shower core expressed in characteristic units of length r/r_1 (at the altitude of 3860 m $r_1 = 125$ m) is plotted along the horizontal axis. The density of non-equilibrium electrons multiplied by r/r_1 is plotted along the vertical axis.

According to these papers the spatial distribution of electrons at the periphery of the shower depends in an essential way on their energy spectrum in the avalanche, and may become quite flat for $S > 1$.

We shall compare the spatial distribution of electrons obtained by us with their distribution in an electron-photon avalanche as calculated by Nishimura and Kamata.¹⁶ Figure 10 shows a theoretical curve¹⁶ which corresponds to the cascade theory parameter $S = 1.0$. A good agreement is observed between the experimental and the theoretical curves over the whole range of distances investigated by us.* We note that the experimental data do not disagree with the theoretical curve for $S = 1.2$. One should thus conclude

*It should be noted that in accordance with Ref. 16, Fig. 10 shows the spatial distribution of electrons of total energy $E > m_e c^2$ while in the experiment a dense substance (counter wall, roof of the building) amounting to 2 gm/cm² is situated above the sensitive volume of the counter, which corresponds to the absorption of electrons of energy < 7 mev. However, since the value of Z for the dense substance is close to that for air the production of electrons by photons compensates for their absorption.

that Coulomb scattering of electrons is by itself sufficient to explain their considerable spatial divergence. The angular divergence of electron avalanches associated with the angles of emission of π^0 -mesons in the elementary events of the nuclear cascade process in this case plays a relatively insignificant role.* We shall now consider the spatial divergence of penetrating particles (μ -mesons) brought about by Coulomb scattering. It depends markedly both on their energy spectrum and on the altitude of the point at which they are produced. An approximate estimate shows that as a result of multiple scattering μ -mesons may reach the periphery of the shower.

Indeed, according to the theory of multiple scattering of charged particles the mean square divergence of particles of energy E which have traversed in the atmosphere a path from the altitude $h_0 + h$ to the altitude h_0 is given, without taking ionization losses into account, by:

$$\overline{r^2}(E) = \int_0^h h'^2 \left(\frac{E_s}{E} \right)^2 \frac{dh'}{L_0 e^{\alpha h'}}, \quad (B)$$

where α is the coefficient in the barometric formula, $\alpha = 1/8000 \text{ m}^{-2}$, L_0 is the value of one radiation length in meters at the altitude h_0 , $E_s = 21 \text{ mev}$.

We substitute into the above formula the average μ -meson energy $E = 10^9 \text{ ev}$ according to Cocconi et al,¹⁵ and their mean altitude of origin of 10,000 m above sea-level according to Bassi et al.¹⁸ Then, for observations carried out at an altitude of 3860 m ($h = 60 \times 10^3 \text{ m}$ and $L_0 = 410 \text{ m}$), we obtain $\sqrt{\overline{r^2}} = 200 \text{ m}$. Concerning the third reason for the divergence of charged shower particles—the earth's magnetic field—it is found to give a deflection

$$r_M(E) = \int_0^H h \frac{dh}{\rho}, \quad \text{where } \rho = \frac{1.1 \cdot 10^{-2}}{\cos \lambda} E; \lambda = 30^\circ \text{ **}$$

On substituting the above values we obtain $r_M = 150 \text{ m}$. We should thus conclude that the Coulomb scattering of μ -mesons and the earth's magnetic field have a pronounced effect on the spatial distribution of μ -mesons. At the same time, it can be easily seen that these causes evidently cannot completely explain the observed divergence of μ -mesons.

* The divergence associated with the influence of the earth's magnetic field does not play any significant role for electrons in electron-photon avalanches as is shown by Cocconi.¹⁷

**The value of the geomagnetic latitude of the station at which our measurements were made.

Indeed, on the basis of the experimental data obtained by us and of the data of Vavilov et al¹¹ we can evaluate:

$$\overline{r^2} = \int r^2 \rho_\mu(r) 2\pi r dr / \int \rho_\mu(r) 2\pi r dr.$$

Such an evaluation gives $\sqrt{\overline{r^2}} > 400 \text{ m}$ ***

This forces us to conclude that the angular divergence of π^\pm -mesons born in elementary events of the nuclear-cascade process also plays a significant role in determining the spatial divergence of μ -mesons.

CONCLUSIONS

In the present work we have carried out a quantitative study of the different components of an extensive atmospheric shower at large distances from its core (200–800 m).

1. The part of the shower which we have studied consists of an electron-photon and a penetrating (apparently a μ -meson) component.

The relative role played by the penetrating component increases considerably as the distance from the shower core increases and at a distance of $r = 800 \text{ m}$ the flux densities of penetrating particles and of electrons become the same. According to Eidus et al,⁵ a similar situation is also observed at sea-level.

2. The spatial distribution of the total flux of electrons and penetrating particles is given by $\rho(r) \sim 1/r^n$ with $n = 3.0 \pm 0.2$.

The spatial distribution of the flux of penetrating particles is given by $\rho(r) \sim 1/r^n$ with $n \approx 2.0$.

3. The relatively slow falling off of the flux densities of shower particles leads to the shower periphery playing an important role in the overall balance of the flux of shower particles. For penetrating particles, this role even becomes the dominant one. Thus a quantitative investigation of the shower cannot be restricted to the study of its central regions as is usually done (see also Ref. 5).

4. The mechanism for the transfer to the periphery of the shower of electrons which are not in equilibrium with μ -mesons is accounted for by the Coulomb scattering of these electrons by nuclei of atoms of air.

5. The transfer to the periphery of the shower of μ -mesons occurs both by means of Coulomb scattering, and apparently also as a result of the large angles of emission in elementary events of the nuclear cascade process of π^\pm -mesons giving rise

***Since the shape of $\rho_\mu(r)$ is known experimentally only up to distances $\sim 800 \text{ m}$ it is clear that we can give only a minimum estimate.

to these μ -mesons.

In the present work we have also obtained data on the intensity of primary cosmic ray particles of ultra high energies of $10^{16} - 10^{17}$ ev by observing extensive atmospheric showers of corresponding energies (with the numbers of particles given by $N = 10^7 - 10^8$): the absolute number of showers with the number of particles $> N$ is given by the expression $F(>N) = AN^{-\alpha}$ where $A = 1 \times 10^{11}$ ($1/m^2$ hour); the index α of the integrated energy spectrum of primary particles in the energy range $10^{16} - 10^{17}$ ev does not exceed 2.15.

In conclusion, the authors wish to express their deep gratitude to N. A. Dobrotin for his assistance in this work, and for valuable advice, and to S. B. Vernov for participating in the discussion of results, and also to D. Parfanovich, Iu. Anishchenko, M. Kazarinova, Iu. Prokhorov, M. Khachaturian, V. Sarantsev, M. Shafranov who all took part in this work in the course of carrying out the practical work for their diplomas, and to E. S. Levit.

1 G. T. Zatsepin and V. V. Miller, J. Exptl. Theoret. Phys. (U.S.S.R.) 17, 939 (1947).

2 D. M. Alekseev, Zatsepin and Morozov, Dokl. Akad. Nauk SSSR 63, 375 (1948).

3 Zatsepin, Kristiansen, and Shuvaev, Report of the cosmic ray laboratory of the Physical Institute of the Academy of Sciences, USSR, 1948.

4 Zatsepin, Rosental', Zakharova, Khrebet and Kristiansen, Dokl. Akad. Nauk SSSR 74, 29, 1950.

5 L. Kh. Eidus et al., J. Exptl. Theoret. Phys. (U.S.S.R.) 22, 440, (1952).

6 J. Blatt, Phys. Rev. 75, 1584, (1949).

7 Zatsepin, Kuchai and Rosental', Dokl. Akad. Nauk SSSR 61, 47 (1948).

8 Cocconi, Tongiorgi-Cocconi and Greisen, Phys. Rev. 75, 1063 (1949).

9 G. B. Kristiansen, Thesis, Moscow, Physical Institute of the Academy of Sciences, USSR (1953).

10 L. N. Korablev, Dokl. Akad. Nauk SSSR 69, 643(1949).

11 Vavilov, Nikol'skii and Tukish, Dokl. Akad. Nauk SSSR 93, 233 (1953).

12 D. V. Skobel'syn, Dokl. Akad. Nauk SSSR 67, 45 (1949).

13 G. T. Zatsepin, Thesis, Moscow, Physical Institute of the Academy of Sciences USSR (1950).

14 I. Molliere. Die kosmische Strahlung, Herausgegeben von W. Heisenberg, Berlin, Springer, (1953).

15 Cocconi, Cocconi-Tongiorgi and Greisen, Phys. Rev. 76, 1020, (1946).

16 L. Nishimura and K. Kamata. Progr. Theor. Phys. 262, 628 (1951). L. Nishimura and K. Kamata. Progr.

of the Int. Conf. of Theor. Phys., Tokio, (1954).

17 J. Cocconi, Phys. Rev. 93, 646; 95, 1705 (1954).

18 Bassi, Klark and Rossi. Phys. Rev. 92, 441 (1953).

Translated by G. M. Volkoff
53